Journal of Sound and Vibration (1983) **91**(1), 135–145

TRANSIENT ACOUSTIC RADIATION FROM IMPACTED BEAM-LIKE STRUCTURES

A. AKAY, M. T. BENGISU† AND M. LATCHA

Department of Mechanical Engineering, Wayne State University, Detroit, Michigan 48202, *U.S.A.*

(*Received* 26 *January* 1982, *and in revised form* 8 *February* 1983)

Transient acoustic radiation from transverse vibrations of beams and beam-like structures is obtained by modelling the structure as a series of contiguous dipoles. A time-dependent expression is developed for sound radiation from a dipole source by Fourier synthesis. Acoustic radiation from the beam is obtained by integrating the sound pressure from the differential dipole elements over the beam length. Time-dependent integration limits are used to account for the transient effects. An analogous discrete formulation is described for beams of arbitrary geometry and density. The radiation patterns of a uniform unbaffled beam are given for frequencies below and above the critical frequency. The results are applied to model the sound radiation from an impact-excited beam.

1. INTRODUCTION

Sound and vibration in mechanical systems have long been a problem of great concern. Requirements for higher productivity and energy efficiency have lead to the design of high-speed machines with lighter moving components. As a result, the problems of vibration, noise, stability, and wear have increased. The dynamic interaction of the flexibility of the light-weight components and the high-intensity impact forces developed in the clearances has become the major source of sound and vibration in high-speed mechanisms.

Sound radiation from mechanisms may be caused by two essential sources. (1) The *aerodynamic sources* in a mechanism are due to instabilities in the air introduced by the motion of the system; rotating fan blades are an example. The radiated sound generated by the aerodynamic sources is related to the shape of the members of the mechanism, and the amplitudes of the sound pressure are proportional to the input speed. (2) The *vibro-acoustic sources* of a mechanism are caused by the vibrations of the members. These vibrations result from inertial forces and impacts due to backlash in the bearings of a mechanism. Vibrations resulting from the inertial forces are at the operating speed of the system and usually have much lower frequencies than those due to impact-excited vibrations.

The dynamic response of links to impact forces can be considered in terms of forced and free vibrations. The axial components of the impact forces in the clearances excite longitudinal vibrations and the vertical components excite transverse vibrations. Axial impacts acting unevenly on the cross-section of the links may also induce transverse and torsional vibrations. An impact force induces a rapid deformation of the impacted object in the immediate vicinity of the contact region, which is followed by the resonant vibrations of the body. During contact, the impacted object may also undergo a rigid-body acceleration if it is unrestrained.

† Present address Silentec Ltd, 785 Plymouth, Suite 304, Mount-Royal, Quebec, Canada.

0022-460X/83/210135+11 $03.00/0

The acoustic radiation characteristics of an impact-excited body follow its vibration response [1]. The axial impact of a link or a beam induces rigid-body radiation due to the acceleration of the whole link where both end surfaces of the beam act like rigid pistons. The rigid-body radiation is followed by the resonant radiation from the beam ends due to its free longitudinal vibrations. In the case of transverse impact of a beam acoustic radiation on the axis of impact consists of a distinct pressure pulse corresponding to the rapid deformation of the contact area which is followed by resonant radiation from the bending vibrations of the beam.

Sound radiation due to free vibrations of a link following impact in most cases dominates over the rigid-body radiation. Then, in the absence of external loads, total acoustic radiation from a link is a result of its forced and free vibrations caused by the impacts in the joints and the lower-frequency inertial forces.

In earlier work on radiation from the transverse vibrations of beams steady state radiation was considered by exact and approximate theories [2–8]. Some of these studies were concerned with baffled beams [2, 3] and in others unbaffled beams of circular [4–6] or elliptical [7, 8] cross sections were modelled. In an extensive analytical and experimental study of radiation from beams of slender elliptical cross section, Blake [8] has obtained expressions for radiated power for baffled and unbaffled beams in air and water and studied the effects of fluid loading. His results suggested that unbaffled beams can be described as an array of dipoles as was done in reference [6].

In this paper, transient radiation from the transverse vibrations of an impacted beam-like link is modelled as a series of contiguous dipoles. An expression for the time-dependent pressure radiation from a dipole with arbitrary vibration response is developed and the acoustic pressure at a point in the field is obtained by considering the phase differences introduced by spatial and temporal distribution of these dipole elements. Effects of resonant radiation below and above the critical frequency are shown by plotting the directivity characteristics of a uniform unbaffled beam.

Since most of the mechanical system elements do not lend themselves to exact closed-form solutions, some form of numerical technique is used to investigate the dynamic behavior of these systems. In the present method use is made of the vibration history obtained by finite element methods to calculate the acoustic field by using the finite beam elements as dipole sources. This procedure is demonstrated for a simple beam and the resulting pressure waveforms are compared with experimental measurements. Effects of the number of beam dipole elements to represent the beam radiation are shown by plotting the pressure contours for different numbers of dipoles.

2. MODELLING OF SOUND RADIATION FROM BEAM-LIKE MEMBERS

Radiation from transverse vibrations of a beam-like member of a mechanism may be modelled as an array of contiguous dipoles by treating each elemental length of the beam or each node of the finite element mesh and the associated transverse surface area as a dipole. Since the vibration characteristics of every node are calculated by solving the vibration problem, it is possible to calculate the resulting sound pressure from each dipole.

2.1. TIME-DEPENDENT SOUND RADIATION FROM A DIPOLE

The sound pressure radiated from a dipole made up of two simple sources of equal strength Q and characteristic dimension a is given by [9]

$$p(r,\theta,\omega)=(\mathrm{j}\rho_0 ck\varepsilon/4\pi r)Q\,\mathrm{e}^{-\mathrm{j}kr}(\mathrm{j}k+1/r)\cos\theta,\qquad \lambda\gg a, \tag{1}$$

where λ is the acoustic wavelength, ε is the distance between the simple sources, $k=\omega/c$ with ω being the circular frequency of the radiation, r is the distance from the center of the dipole to the receiver point, and θ is the angle from the plane of symmetry between the simple sources. ρ_0 and c are the density and the speed of sound in the surrounding medium.

The strength of the source in the frequency domain can be written as

$$Q(\omega)=Su(\omega), \tag{2}$$

where S is the surface area and u is the surface velocity. Then the steady state acoustic radiation from a dipole vibrating with a velocity $u(\omega)$ can be expressed from equation (1) as

$$p(r,\theta,\omega)=(\rho_0 S\varepsilon/4\pi r)u(\omega)\,\mathrm{e}^{-\mathrm{j}kr}[(1/c)(\mathrm{j}\omega)^2+(1/r)(\mathrm{j}\omega)]\cos\theta. \tag{3}$$

For an arbitrary velocity, $u(\omega)$, the pressure-time history can be obtained from equation (3) by Fourier synthesis [10]:

$$p(r,\theta,t)=\frac{\rho_0 S\varepsilon}{4\pi r}\cos\theta\,\frac{1}{2\pi}\int_{-\infty}^{\infty}\left[\frac{1}{c}(\mathrm{j}\omega)^2+\frac{1}{r}(\mathrm{j}\omega)\right]u(\omega)\,\mathrm{e}^{-\mathrm{j}\omega r/c}\,\mathrm{e}^{\mathrm{j}\omega t}\,\mathrm{d}\omega. \tag{4}$$

By utilizing the shift theorem in Fourier transforms, equation (4) can be written as

$$p\left(r,\theta,t+\frac{r}{c}\right)=\frac{\rho_0 S\varepsilon}{4\pi r}\cos\theta\frac{1}{2\pi}\int_{-\infty}^{\infty}\left[\frac{1}{c}(\mathrm{j}\omega)^2+\frac{1}{r}(\mathrm{j}\omega)\right]u(\omega)\,\mathrm{e}^{\mathrm{j}\omega t}\,\mathrm{d}\omega. \tag{5}$$

Multiplication of the integrand by $\mathrm{j}\omega$ corresponds to taking its derivative with respect to time; therefore, equation (5) becomes

$$p\left(r,\theta,t+\frac{r}{c}\right)=\frac{\rho_0 S\varepsilon}{4\pi r}\cos\theta\left(\frac{1}{c}\frac{\partial^2}{\partial t^2}+\frac{1}{r}\frac{\partial}{\partial t}\right]\frac{1}{2\pi}\int_{-\infty}^{\infty}u(\omega)\,\mathrm{e}^{\mathrm{j}\omega t}\,\mathrm{d}\omega. \tag{6}$$

The integral in equation (6) is the Fourier transform of $u(t)$, which is given by

$$u(t)=\frac{1}{2\pi}\int_{-\infty}^{\infty}u(\omega)\,\mathrm{e}^{\mathrm{j}\omega t}\,\mathrm{d}\omega.$$

Then equation (6) becomes

$$p(r,\theta,t+r/c)=(\rho_0 S\varepsilon/4\pi r)[(1/c)\partial^2 u(t)/\partial t^2+(1/r)\partial u(t)/\partial t]\cos\theta. \tag{7}$$

Upon shifting the time co-ordinates once again, equation (7) takes the form

$$p(r,\theta,t)=\frac{\rho_0 S\varepsilon}{4\pi}\left[\frac{1}{cr}\frac{\partial^2 u(t-r/c)}{\partial t^2}+\frac{1}{r^2}\frac{\partial u(t-r/c)}{\partial t}\right]\cos\theta. \tag{8}$$

Equation (8) gives the time-dependent sound radiation from a dipole with arbitrary surface acceleration. In equation (8), the term $(1/r^2)\partial u(t-r/c)/\partial t$ represents the near field radiation and loses effectiveness in the far field where the term $(1/cr)\partial^2 u(t-r/c)/\partial t^2$ becomes dominant.

2.2. TRANSIENT RADIATION FROM AN ARRAY OF DIPOLES

Total acoustic pressure at any field point resulting from an array of dipoles can be found by summation of the contributions of individual dipoles at this point. Sound pressure at a point (r,θ,ψ) from each element of an array of dipoles can be written in the frequency domain, by using equation (3), as

$$p(r,\theta,\psi,\omega)=(\rho_0 S\varepsilon(x)/4\pi r')u(x,\omega)\,\mathrm{e}^{-\mathrm{j}kr'}[(1/c)(\mathrm{j}\omega)^2+(1/r')(\mathrm{j}\omega)]\cos\theta\sin\psi, \tag{9}$$

and in the time domain, from equation (8), as

$$p(r,\theta,\psi,t)=\frac{\rho_0 S\varepsilon(x)}{4\pi r'}\left[\frac{1}{c}\frac{\partial^2 u(x,t-r'/c)}{\partial t^2}+\frac{1}{r'}\frac{\partial u(x,t-r'/c)}{\partial t}\right]\cos\theta\sin\psi, \tag{10}$$

where the axis of the dipole array coincides with the x axis ($\theta=\pi/2$, $\psi=\pi/2$) and r' is the distance from each dipole to the receiver point as shown in Figure 1.

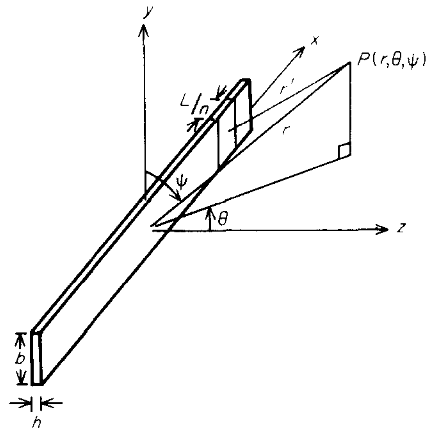

Figure 1. The geometry of the problem.

In the case of a continuous array of dipoles, such as a transversely vibrating thin beam, the sound pressure at a field point can be found by considering the beam as an array of infinitesimal dipoles with differential surface areas $S=b(x)\,\mathrm{d}x$, where $b(x)$ is the non-uniform beam width. Sound pressure at a point (r,θ,ψ) is obtained by integrating the differential pressure expression for elemental dipoles over the length of the beam. Then the total pressure in the frequency domain is

$$p(r,\theta,\psi,\omega)=\frac{\rho_0}{4\pi}\cos\theta\sin\psi\int_L b(x)\varepsilon(x)u(x,\omega)\left[\frac{1}{r'c}(\mathrm{j}\omega)^2+\frac{1}{r'^2}(\mathrm{j}\omega)\right]\mathrm{e}^{-\mathrm{j}kr'}\,\mathrm{d}x, \tag{11}$$

and in the time domain is

$$p(r,\theta,\psi,t)=\frac{\rho_0}{4\pi}\cos\theta\sin\psi\int_L b(x)\varepsilon(x)\left[\frac{1}{r'c}\frac{\partial^2 u(x,t-r'/c)}{\partial t^2}+\frac{1}{r'^2}\frac{\partial u(x,t-r'/c)}{\partial t}\right]\mathrm{d}x, \tag{12}$$

where $r'=[x^2-2xr\sin\psi\sin\theta+r^2]^{1/2}$ is the distance from the receiver point to each differential dipole element.

For steady state radiation problems the integrals in equations (11) and (12) are carried out over the length of the beam. Time delay in the arrival of sound waves at the receiver point due to differences in distance from the dipole elements along the beam is taken into account by the phase-shift term $\exp(-\mathrm{j}kr')$ or by the time-delay term $(t-r'/c)$ in equations (11) and (12), respectively. In the case of transient radiation problems, the integral limits in equation (12) must be time-dependent to account for the additional phase-shift introduced by the earlier arrival of sound waves from closer parts of the beam at the start of radiation. Similarly, time-dependent integral limits are used at the conclusion of a transient radiation to allow for the late arrival of the sound waves from the distant parts.

Acoustic radiation from a beam with complex shape and arbitrary vibration response can be found by numerically integrating the integral in equation (12). In cases where the complex vibratory response of a beam or beam-like element is obtained at discrete points by using numerical techniques, the corresponding acoustic radiation can be obtained by summation of the pressure from each of these discrete dipole elements that make up the beam.

In the study described here, transient sound radiation from an impact-excited beam was obtained by using a finite number of dipole sources representing the beam. The total sound pressure at a point (r, θ, ψ) at time t this was obtained by summation of the sound pressure from each dipole element with appropriate time delay,

$$p(r, \theta, \psi, t) = \sum_{i=1}^{n} p_i(r_i, \theta_i, \psi_i, t_i'), \qquad t > r_{\min}/c, \tag{13}$$

where n is the number of dipoles used to represent the beam, $t' = t - r_i/c$, p_i and r_i are the sound pressure and the distance from dipole element i to the receiver point, and $r_{\min}$ is the smallest value of r_i.

As discussed earlier, in transient radiation problems, initially the limit of summation in equation (13) is determined from the geometry of the source array and the receiver point and the delay time between these points. After time $t = r_{\max}/c$ all n dipoles contribute to the total sound pressure.

2.3. RADIATION PATTERNS OF AN UNBAFFLED FINITE BEAM

Acoustic radiation from a finite beam is better approximated with a higher number of dipoles in the present model. The number of dipoles used determines the frequency range of the model, and must be equal to or larger than the number of the highest mode of interest. In addition, since the beam segments are represented by rigid pistons, using a higher number of dipoles provides a closer approximation of the beam curvature. From the analysis in reference [8], the distance ε between the simple sources of the dipoles is found to be $\varepsilon = b/2{\cdot}55$, where b is the width of the beam. The dependence of ε on beam width follows from the definition of dipoles which are used to model force fluctuations. In the present case, the forces acting on the surrounding medium of an elemental beam length due to its transverse vibrations are effected primarily by the beam width rather than by its thickness.

Steady state radiation from a simply supported beam at its mth mode can be written as

$$\frac{p_m(r, \theta, \psi, t)}{\rho_0 A\varepsilon/4\pi} = \sin\psi \sum_{i=1}^{n} S_i \cos\theta_i \left\{\frac{\omega_m}{r_i c}\sin\left[\omega_m(t - r_i/c)\right] - \frac{1}{r_i^2}\cos\left[\omega_m(t - r_i/c)\right]\right\}\left\{\begin{matrix}\sin(m\pi/L)x_i, & m \text{ even} \\ \cos(m\pi/L)x_i, & m \text{ odd}\end{matrix}\right\}, \tag{14}$$

where x varies between $-L/2$ and $L/2$, and the co-ordinates are measured from the geometric center of the beam. S_i is the surface area of each dipole element and A is the acceleration amplitude of the beam vibrations. Loci of the sound pressure calculated from equation (14) have been plotted for different modes of a 24 cm × 1.5 cm × 0·7 cm steel beam to show radiation directivity along its length. Figure 2 shows the directivity patterns for the first to the sixth mode as obtained by using one to six dipoles, respectively. For comparison purposes, radiation from the sixth mode is plotted in Figure 3 as obtained by using three, 12 and 24 dipoles, and the results are compared with the directivity pattern obtained by using equation (12). It is apparent that using a number of dipoles

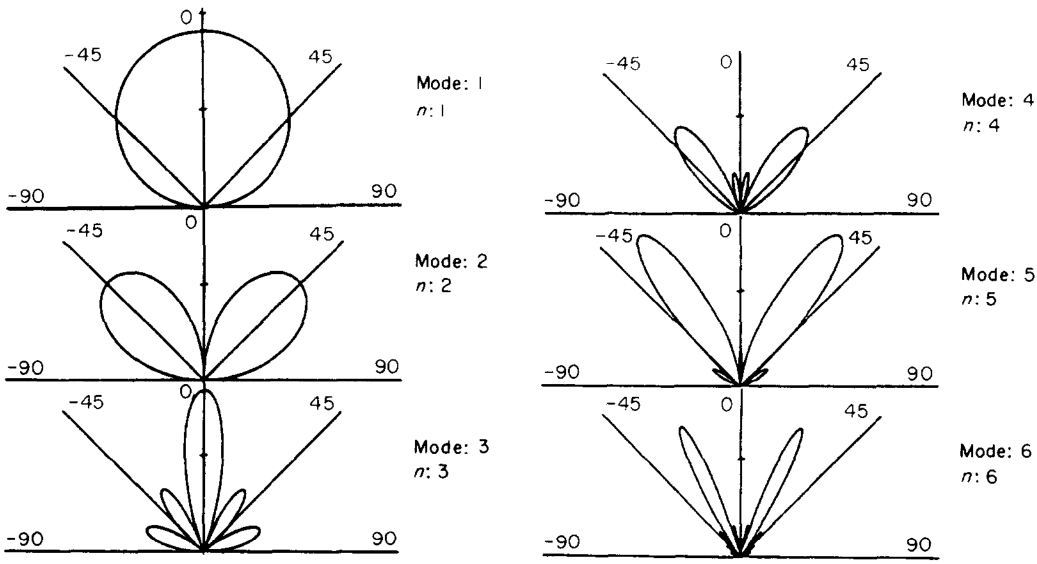

Figure 2. Sound radiation pattern of a beam at different modes at $R/L = 4$. n = number of dipoles.

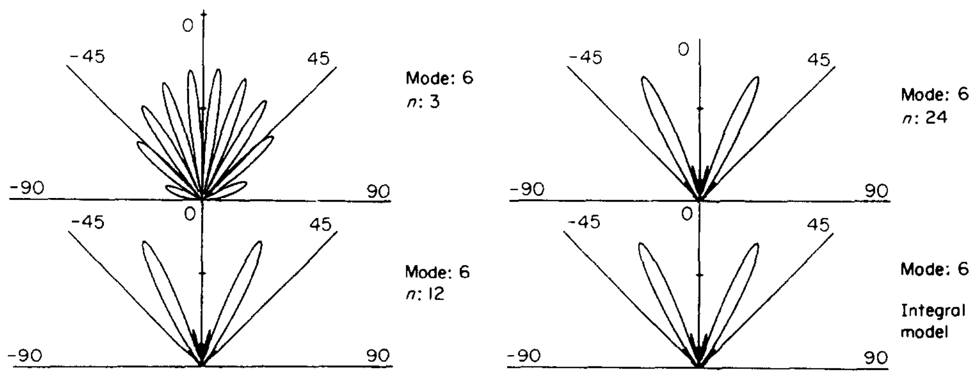

Figure 3. Sound radiation pattern of a beam at its sixth mode modelled with 3, 12 and 24 discrete dipoles, and by continuous integral (equation (12)).

less than the mode number is inadequate. For the correct prediction of directivity and the amplitude, the number of dipoles must be equal to or larger than the highest mode number of interest. Increasing the dipole number further gives results closer to those obtained from the integral equations (11) and (12), but without substantial improvement. Directivity patterns for the second and fifth modes are given in Figures 4(a) and (b) for different distances. An apparent difference is the change of the directivity characteristics of these modes with distance which will be discussed further.

3. ACOUSTIC AND VIBRATION RESPONSE OF AN IMPACTED BEAM

3.1. VIBRATION RESPONSE

Flexural vibrations of a beam-like member of a mechanism resulting from impact forces in the joints can be obtained analytically with finite elements. The number of

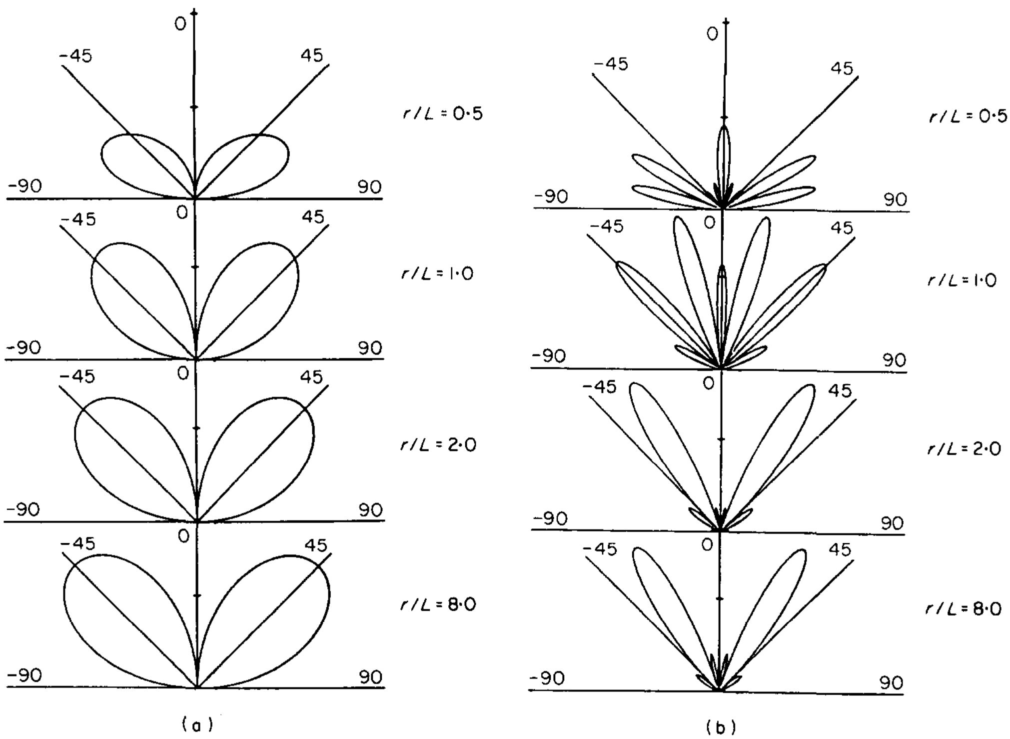

Figure 4. Radiation pattern for the (a) second mode and (b) fifth mode of the beam at different distances.

nodes selected to represent the beam determines the number of eigenmodes and the spectral accuracy of the resulting sound pressure field.

The present transient vibration problem requires solving a second-order time-dependent non-homogeneous matrix differential equation [11],

$$[M]\{\ddot{x}(t)\}+[C]\{\dot{x}(t)\}+[K]\{x(t)\}=\{F(t)\}, \tag{15}$$

where $\{x(t)\}$, $\{\dot{x}(t)\}$ and $\{\ddot{x}(t)\}$ are displacement, velocity and acceleration vectors, $\{F(t)\}$ is the time-dependent force vector, and $[M]$, $[C]$ and $[K]$ are the mass, damping and stiffness matrices constructed by the finite element method, which can be found in standard textbooks on finite elements [11]. The values of $[M]$ and $[K]$ depend on the material and geometry of the beam. The value for the equivalent damping coefficient was measured for each beam. The force vector $\{F(t)\}$ is made up of the impact forces and the unknown reaction forces at the supports. The reaction forces and the corresponding differential equations are excluded from the matrix equation (15).

The time-dependent coupled differential equations (15) have been solved numerically by using the Newmark Method [12]. During the contact period the acceleration was calculated from the impact force values at each time step. After the impact force ceased average acceleration was used.

3.2. IMPACT FORCES

The impact forces can be calculated by using Hertz contact theory [13] for the cases of impact of a spherical object on a flat body and for the impact of a pin and socket [14]. The impact force developed between a sphere and a flat surface can be described as

$$F(t) = k_2 \alpha(t)^{3/2}, \tag{16}$$

where $\alpha(t)$ is the relative approach of the center of gravity of the impacting bodies during contact and is described by:

$$\alpha(t) = \alpha_m \sin(\pi/\tau)t,$$

where α_m is the maximum value of $\alpha(t)$ and is equal to $\alpha_m = [5u_0^2/4k_1k_2]^{0\cdot 4}$ for an impact velocity u_0. The contact duration τ is described by

$$\tau = 2\cdot 9432\ \alpha_m/u_0.$$

The quantities k_1 and k_2 depend on the material properties and geometric configurations of the impacting objects. For the impact of a spherical object on a flat body [13], $k_1 = 1/m$ and $k_2 = 4\sqrt{a}/3\pi(\delta_1+\delta_2)$, where m is the mass of the sphere of radius a.

For the impact of a pin in a socket, the relationship between the force and the approach, α, is given in reference [14] as

$$\alpha = F\{\ln[(r_1 - r_2)8a^3\,\mathrm{e}/r_1r_2(\delta_1+\delta_2)] - \ln F\}[(\delta_1+\delta_2)/2l], \tag{17}$$

where r_1, r_2 are the pin and socket diameters, $2l$ is the length of the pin in the connection, and e is the natural logarithm base. The material properties δ_1 and δ_2 depend on the elasticity modulus E, and on Poisson's ratio μ of the ball and flat body or pin and socket, respectively: $\delta = (1-\mu^2)/\pi E$. Equation (17) has been used with reference [15] to obtain the forces developed in the pin connection due to impacts.

4. EXPERIMENTS

A set of experiments was designed to measure the sound pressure waveforms from beams corresponding to the theoretical analysis presented. All the sound pressure measurements were made in an anechoic chamber using a $\frac{1}{2}$ inch diameter free-field microphone.

Transient radiation waveforms were measured by impacting a simply supported $1\cdot 1$ m $\times$ $0\cdot 032$ m $\times$ $0\cdot 0095$ m aluminum beam at its mid-point by a $1\cdot 9$ cm diameter Plexiglass ball. Acceleration response of the beam was measured on the opposite side of the beam from the impact point using a subminiature accelerometer. Pressure waveforms were obtained using a storage oscilloscope triggered by the acceleration signal.

A specially designed experimental four-bar mechanism was used to measure the sound pressure waveforms corresponding to the theoretical prediction of radiation. For clearances in the joints of the mechanism less than 10 μm, the sound and vibration responses of the links were not appreciable except at the low operational frequency of the mechanism. However, a larger clearance was set up at the ground–rocker joint to generate impact of the pin in the sleeve bearing, causing higher frequency vibrations and sound radiation from the rocker. The resulting intermittent transient waveforms were measured at a distance of $0\cdot 5$ m in the direction of motion of the rocker.

5. RESULTS

The theoretical vibration response corresponding to the simply supported aluminum beam impacted by a $1\cdot 90$ cm diameter Plexiglass sphere was obtained by a finite element method with 18 elements. The impact force was computed by using the Hertz theory described earlier. The resulting transient radiation from the beam was calculated by using equations (10) and (15). An example of the computed and measured sound pressure waveforms at the point $P(1\ \mathrm{m}, 0°, 90°)$ are given in Figures 5(a) and (b), respectively. The time increment used in this computation was 50 μs. Larger values for the time increment resulted in distortions of the pressure waveform. The initial pulse starting at time zero in Figures 5(a) and (b) is the radiation due to forced deformation of the beam during impact which precedes the radiation due to free vibrations of the beam.

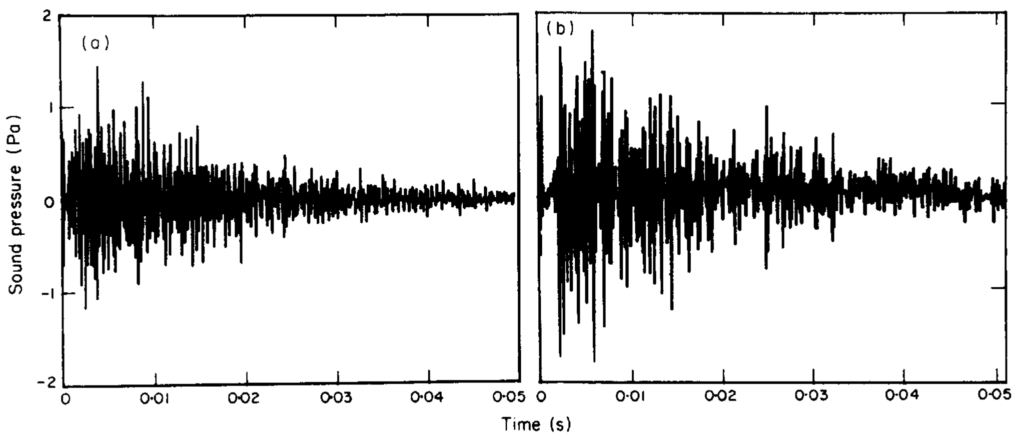

Figure 5. Transient sound pressure at point P (1 m, 0°, 90°) (a) calculated with 50 μs time increments; (b) measured.

Similar theoretical pressure waveforms were obtained for the rocker of a four-bar mechanism with a clearance at the ground–rocker joint. Impact force direction and magnitude and the transverse vibration response of the rocker were computed as described in section 3. The computed and measured waveforms at the point P (0·5 m, 0°, 90°) are shown in Figures 6(a) and (b) for a crank speed of 500 rpm.

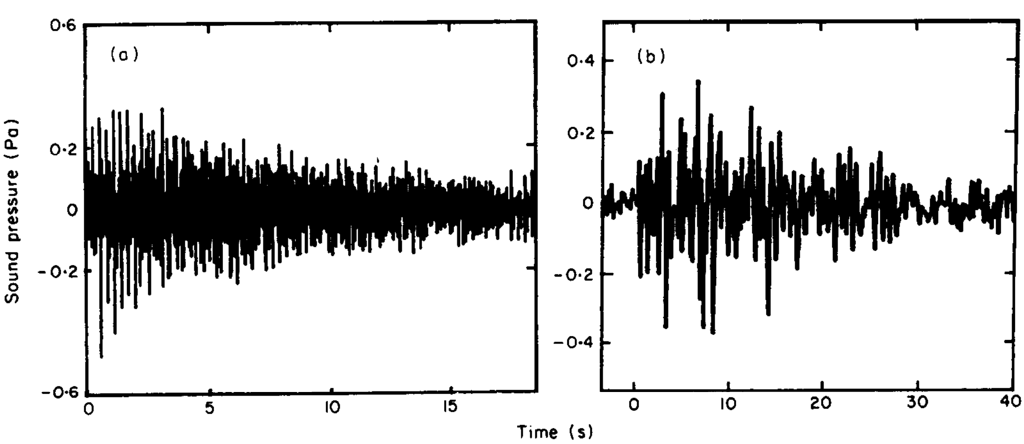

Figure 6. Transient sound pressure radiation from the follower at 500 rpm, at point P (0·5 m, 0°, 90°). (a) Calculated; (b) measured.

6. DISCUSSION AND CONCLUSIONS

Directivity patterns of a simply supported unbaffled beam are shown in Figures 2–4. In Figure 2, the directivity patterns for the first two modes correspond to one and two out-of-phase dipoles, respectively. Each dipole represents radiation from each half-wavelength of the beam. Above the third mode radiation configurations show two primary lobes from each side of the beam. This directivity pattern follows the general radiation characteristics from bending waves of a beam. Below the critical frequency f_c the radiation pattern for each mode of a finite unbaffled beam displays a number of lobes from each side of the beam equal to the mode number of beam resonance. The interference patterns of the pressure waves from various parts of the beam do not change appreciably with distance from the beam, as shown in Figure 4(a). Above the critical frequency, the radiation mechanism is different and the pressure waves have preferred directions. Radiation at any mode above the critical frequency shows two primary lobes at each side of the beam. The direction of these lobes can be found from $\theta = \pm\sin^{-1}(c/c_B)$ where c_B is the speed of bending waves of the beam. The computed values of θ and the corresponding values in Figure 2 are in excellent agreement. The analogy of the radiation characteristics between finite beams and infinite beams or plates becomes apparent when the standing waves in the resonant modes of a beam are considered as two bending waves traveling in opposite directions, thus radiating sound as in infinite beams or plates. Unlike radiation patterns below the critical frequency, directivity above f_c shows significant changes with distance as shown in Figure 4(b), indicating a strong reactive field near the beam.

In this paper acoustic radiation from transverse vibrations of non-uniform beams and beam-like structures has been modelled by representing the beam as an array of contiguous dipoles. A time-dependent expression was developed for steady state and transient radiation problems. Both a continuous dipole array model, with an integral expression, and a discrete model, with a finite number of dipoles, have been developed. It was shown that for a number of discrete dipoles higher than the highest mode number these models agree with each other. The general waveform characteristics and the pressure amplitudes from the analytical models and the measurements also agree reasonably well.

The dipole modelling of transverse vibrations is strictly valid for vibrating objects of small cross section in terms of the acoustic wavelength, such as strings. In cases of beams of slender cross section, dipole modelling is a good approximation of the acoustic radiation provided that the cancellation effects of the dipoles is not strongly affected by the beam width. In reference [8] a good discussion of the limitations due to width effects is given and it was shown that the dipole source strength is primarily determined by the beam width. The analytical results in reference [8] also show that the characteristic dimension of the dipole, $\varepsilon/2$, is equivalent to approximately one-fifth of the beam width.

In the present model both the near and far field terms of the dipoles have been included. The effect of distance on the radiation pattern is shown in Figures 4(a) and (b) for the second and fifth modes. Radiation from the fifth mode converges to two major lobes at distances $r/L \geqslant 4$. The second mode shows only minor changes in direction with distance.

The models presented here can be used as a design tool to obtain the radiated acoustic power from complex shaped slender beams excited by transient forces.

ACKNOWLEDGMENT

The authors wish to acknowledge their gratitude to the National Science Foundation's Mechanical Systems Program for the support of this study under Grant No. CME79-21242, and would like to thank the reviewers for their valuable comments.

REFERENCES

1. A. AKAY 1978 *Journal of the Acoustical Society of America* **64**, 977–987. A review of impact noise.
2. R. H. LYON and G. MAIDANIK 1962 *Journal of the Acoustical Society of America* **34**, 623–639. Power flow between linearly coupled oscillators.
3. C. E. WALLACE 1972 *Journal of the Acoustical Society of America* **51**, 936–945. Radiation resistance of a baffled beam.
4. J. R. BAILEY and F. J. FAHY 1972 *Journal of Engineering for Industry* **94**, 139–147. Radiation and response of cylindrical beams excited by sound.
5. S. N. YOUSRI and F. J. FAHY 1973 *Journal of Sound and Vibration* **26**, 437–439. Sound radiation from transversely vibrating unbaffled beams.
6. M. C. JUNGER 1972 *Journal of the Acoustical Society of America* **52**, 332–334. Sound radiation by resonances of free–free beams.
7. R. A. JOHNSTON and A. D. S. BARR 1969 *Journal Mechanical Engineering Science* **11**, 117–127. Acoustic and internal damping in uniform beams.
8. W. K. BLAKE 1974 *Journal of Sound and Vibration* **33**, 427–450. The radiation from free–free beams in air and in water.
9. L. E. KINSLER and A. R. FREY 1962 *Fundamentals of Acoustics*. New York: John Wiley and Sons, Inc.
10. A. AKAY 1981 (unpublished). A note on transient radiation from a rigid piston in an infinite baffle.
11. K. H. HUEBNER 1975 *The Finite Element Method for Engineers*. New York: John Wiley and Sons, Inc.
12. K. J. BATHE and E. L. WILSON 1976 *Numerical Methods in Finite Element Analysis*. New York: Prentice–Hall, Inc.
13. W. GOLDSMITH 1960 *Impact*. London: Edward Arnold (Publishers) Ltd.
14. S. DUBOWSKY and F. FREUDENSTEIN 1971 *Journal of Engineering for Industry* **93**, 305–309. Dynamic analysis of mechanical systems with clearances.
15. S. TIMOSHENKO and J. N. GOODIER 1970 *Theory of Elasticity*. New York: McGraw-Hill Book Company, third edition. See Chapter 12.